FINAL REPORT: MARIE CURIE ACTIONS – IEF

Project Acronym: STEM-Activation (n° 332317)

Proposal title: Perivascular meningeal stem cells: a new player in the Neurovascular Unit. Characterization, modulation and therapeutic potential of perivascular meningeal stem cell activation in neurological disorders

Researcher: Ilaria Decimo

As it was described in the project plan, I focused my work on the characterization and modulation of the meningeal stem perivascular cell (MeSP) activation and differentiation. I also evaluated the metabolic profile of the MeSP and the in vitro role of candidate metabolic key modulators (i.e. PFKFB3) in MeSP activation/differentiation. In order to select the best transgenic mice to trace MeSPs *in vivo*, I screened different CRE (PDGFrß, Wnt1) and CRE inducible (SOX10, Nestin, Glast, PDGFralpha) reporter lines intercrossed with Rosa26-lox-stop-lox-YFP mice. During this screening I was particularly interested the PDGFrß-Cre:YFP line. The PDGFRß-Cre:YFP mouse lines showed high recombination in the perivascular cells of either the meninges and the brain as expected, however YFP expression is also present in the choroid plexi and in brain parenchyma neurons. Those findings suggest a possible contribution of MesP to neurogenesis *in vivo*. The in *vivo* identity and fate of MesP is still largely unknown and the hypothesis of the presence of neurogenic cells in meninges would challenge the dogma that only parenchymal cells can contribute to neurogenesis, highlighting the importance of vascular cells as a reservoir of neurogenic cells. Given the potential breakthrough of this hypothesis we focus the project into more detail on the contribution of MeSP to neurogenesis *in vivo*. The results obtained are described below and in the **DEVIATIONS** section.

SUMMARY PROGRESS TOWARDS OBJECTIVES

I first characterized the MeSP migration ability and chemotaxis in response to different candidate molecules. To this aim I cultured meningeal cell extracts from postnatal day (P) 0 mice. After 1 week in culture they generate neurospheres that can be expanded for several passages. In these culture conditions MeSP proliferate and migrate. By using a Boyden Chamber assay, I explored the migration response of MeSP to SDF1a, SDF1b, SEMA3A and SEMA3F (Fig. 1) at different concentrations (1ng/ul, 0,1ng/ul and 0,01 ng/ul).

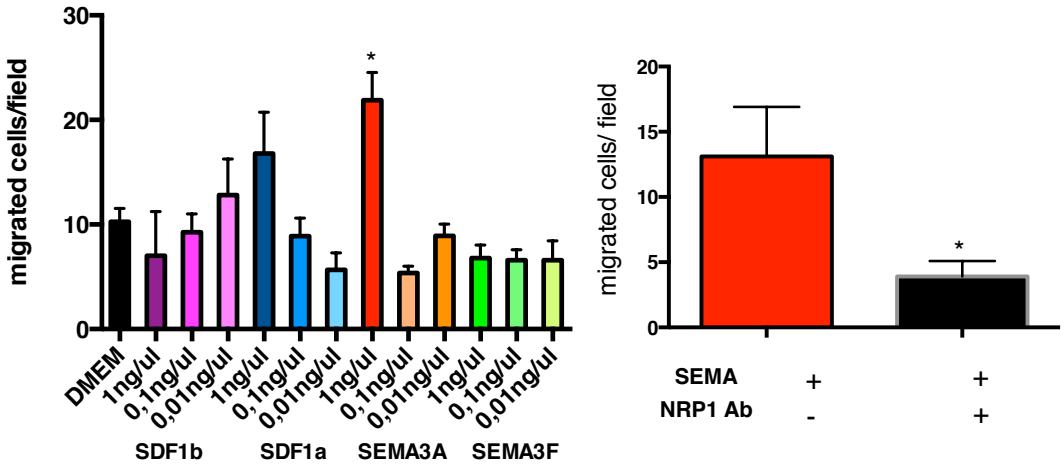

Figure 1: Boyden chamber migration assay of active MeSP. MeSP were seeded on 8,0um filter and exposed to different chemoattractant at different concentrations. Migration was assessed after 16hrs. SEMA3A showed a statistically significant ($p<0,05$) effect on MESP migration. SEMA3A effect on migration could be blocked by a neuropilin antibody.

I could demonstrate that MeSP significantly increased their migration capability in response to SEMA3A. The increased migration in response to SEMA3A was blocked by a neuropilin1 antibody (Fig.1b), suggesting that MeSP chemotaxis was driven by the SEMA3A and neuropilin1 receptor interaction. As I observed variability in migration and chemotaxis properties between different samples of MeSP in culture, I'm performing other techniques to further confirm these results. Therefore, I am using sorted PDGFRß$^{+}$ MeSP and WNT1CRE derived YFP+ MeSP.

As a next step, I assessed the multipotent MeSP differentiation potential *in vitro* (Fig. 2). Indeed MeSP can be successfully differentiated into MAP2+neurons and PDGFrß$^{+}$ pericytes.

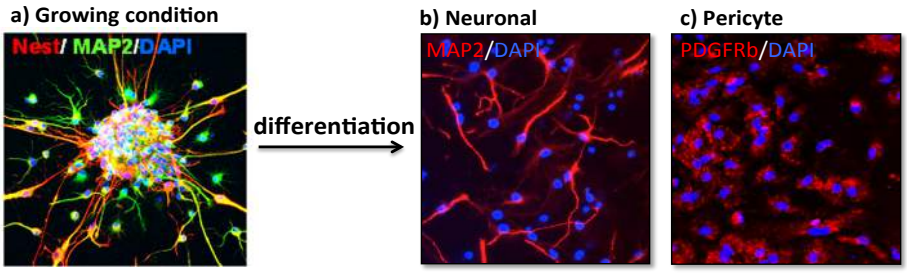

Figure 2: MesP in growing condition form neurospheres expressing the neural and stem cell markers (nestin and MAP2). Changing the medium conditions they can be induced to differentiate into neurons and pericytes.

Taking advantage of the extensive expertise on cell metabolism in the host lab, I have profiled the MeSP metabolism in stemness and differentiating conditions by using radioactive tracers. The rationale for this analysis is that targeting the energy metabolism could be an innovative strategy to induce endogenous stem cell differentiation [1]. Indeed, stemness can be regulated by energy metabolism and differences in energy status can distinguish stem cells from differentiated cells [1]. I measured glucose oxidation (1-14C-glucose), glutamine (Q) oxidation (U-14C-Q), fatty acid oxidation (U-14C-palmitate) and the pentose phosphate pathway (1-14C-glucose oxidation vs 6-14C-glucose oxidation). The results showed a clear shift from glycolytic to oxidative metabolism in growing *vs* differentiated cells. Interestingly, neuronal differentiation of MeSP was, as expected, characterized by increased glutamine oxidation, while pericyte differentiation was associated with an increase in fatty acid oxidation (Fig. 3). I also measured the OCR oxygen consumption which was increased in differentiated cells.

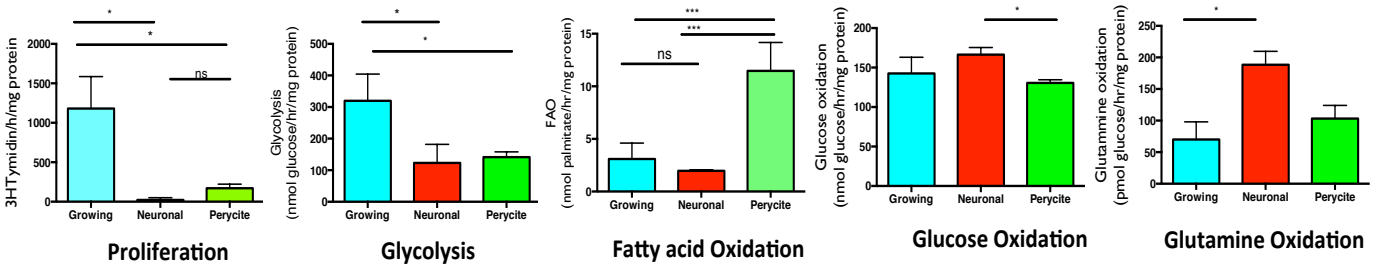

Figure 3: Metabolic analysis of growing and differentiated (neuronal and pericyte) MeSP by using 3H thymidine (proliferation), 5-^{3}H-glucose 9 (glycolysis), 10-^{3}H-palmitate (fatty acid oxidation, FAO) 1-^{14}C D-Glucose 6-^{14} vs C D-Glucose (glucose oxidation) and U-14C-Q (glutamine oxidation) radioisotope tracers. (* p<0,05; ***p<0,0005)

The host lab has shown that PFKFB3 is a key metabolic regulator of glycolysis in vascular endothelial cells (ECs) [2]. Therefore, I hypothesized that PFKFB3 is an important regulator of glycolysis in MeSP cells, and that glycolysis is necessary to activate (e.g. increase in proliferation and migration) perivascular meningeal stem cells and to modulate their differentiation. In order to test this hypothesis I silenced MeSP by using a lentiviral shPFKFB3 construct. I compared the gene expression of neural

stem cell markers and PFKFB3 of transduced and control growing MeSP neurospheres. Interestingly, I found that the expression of neural precursor genes (dcx and tubulinB3) was decreased in PFKFB3 silenced MeSP. On the contrary, the stemness related gene nestin slightly increased. PFKFB3 expression was reduced as expected.

I further determined the effect of PFKFB3 knock down on the MeSP neural differentiation potential. Following MeSPs transduction with lentiviral shPFKFB3 construct, I obtained about 60% of PFKFB3 knock down. In neuronal differentiating conditions I observed a decrease in branching of MAP2 positive cells derived from silenced MeSP compared to control (Fig. 4).

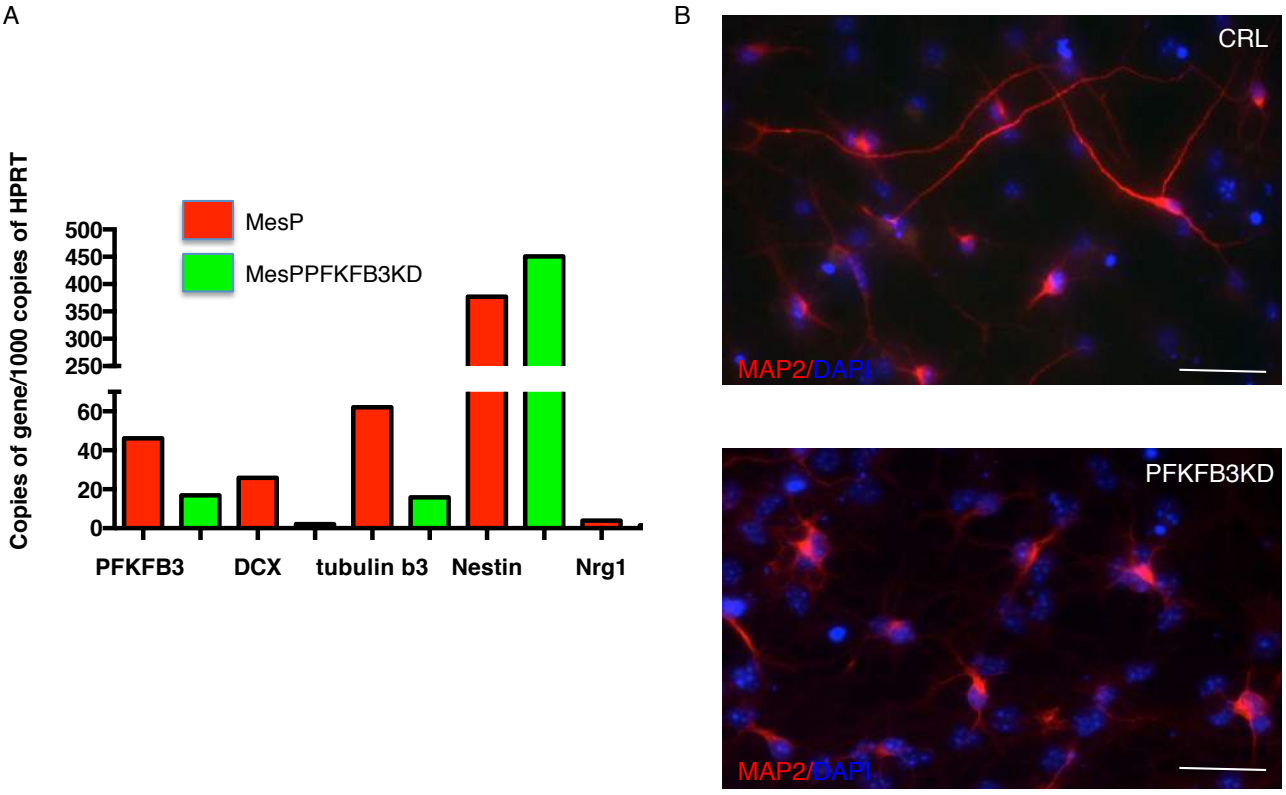

Figure 4: A) RT-PCR analysis of shPFKFB3 and control MeSP neurospheres for neural-stem cell related genes. B) Neural differentiation of PFKFB3KD MeSP vs control MesP. n=1 qPCR, n=3 immunoflurescence. Scale bars are 50μm.

These data are still preliminary and more confirmation experiments are ongoing, however they confirm the hypothesis of testing the in vivo effect of PFKFB3 knock down in MeSP. To this aim I have crossed transgenic mouse lines expressing Cre-recombinase from the locus PDGFRbeta and NG2 (highly expressed in meninges) with lox/lox PFKFB3 mouse lines. Those mice gave their first litter in March and May of this year respectively. I already scheduled in vivo experiments with those animals.

As meningeal perivascular cells are derived from a heterogeneous cell population, I have set up experiments to isolate and sort cells from the meninges of WNT1-YFP mice. With this approach I obtained from total meningeal extract of Wnt1-YFP transgenic mice 13%± 4.7 of YFP^{+} cells. Wnt1 derived MeSP in culture can give rise to neurospheres and differentiate into neurons and pericytes. I plan to confirm this result and to complete the metabolic studies on Wnt1-YFP derived cells.

DEVIATIONS

In addition to the originally proposed experiments investigating MeSP activation, their metabolic profile

and the effect of their metabolism modulation in pathological conditions, I have added experimental investigations to determine the MeSP identity, their possible contribution to neurogenesis and their developmental origin. MeSP contribution to neurogenesis is a largely unexplored field and it would open completely new prospective in the field of neurogenesis and regenerative therapies. The results of this work are under revision in Science (Decimo et al. Perivascular meningeal cells contribute to cortical neurogenesis in the mammalian brain).

I first employed gene fate mapping using mouse strains expressing Cre recombinase from the locus PDGFRß highly expressed in meningeal perivascular cells, We crossed a PDGFRbeta-Cre driver line with a Rosa26-lox-stop-lox-YFP reporter mouse line, thus resulting in recombination and subsequent permanent YFP expression of the PDGFRß$^{+}$ expressing cells. As expected, the PDGFRß-YFP mouse lines showed high recombination in the perivascular cells of either the meninges and the brain (Fig. 5 A-C). In addition, I observed YFP expression in the choroid plexi (Fig. 5 B). Interestingly, I also found recombined YFP^{+} neurons in brain parenchyma postnatal day (P) 0. Although, I cannot exclude recombination events early in the development, these data support the idea that neural cells may derive from PDGFRß expressing cells.

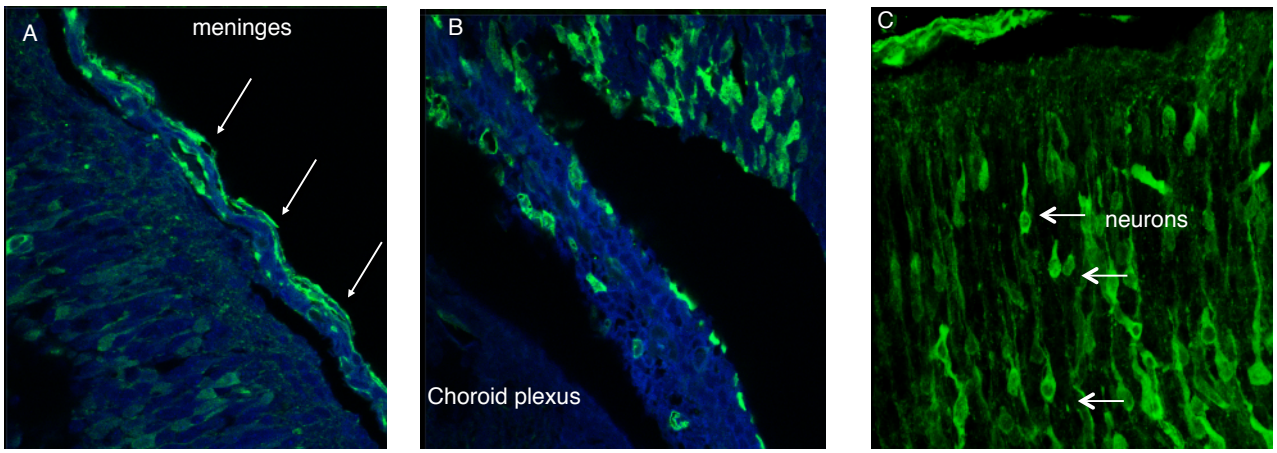

Figure 5: PDGFRß-YFP brain at P0 stage. YFP positive cells are present in meninges choroid plexi and cortical neurons (A, B, C).

We explored **the hypothesis that perivascular cells in the meninges outside the brain parenchyma are able to generate neural cells *in vivo***. To test this hypothesis, we used a technique to selectively transfect only meningeal and not cortical parenchymal cells, by electroporating a red fluorescence protein (RFP) reporter plasmid into the meninges (Fig. 6A). In contrast to other gene transfer techniques (i.e. lentiviral vector), plasmid electroporation allows rapid detection of transfected cells within hours, but only for a limited period. Indeed, RFP electroporation in meninges of newborn (P0) wild type mice resulted in specific labeling of meningeal cells 8 hours later, without however labeling cortical cells (Fig. 6B). At 24 to 48 hours after electroporation, radially oriented RFP^{+} cells were detected in the ventricular and subventricular zone (Fig. 6C), suggesting that these transduced meningeal cells had migrated into the brain parenchyma. When performing a time course analysis to define the migration path of the electroporated cells, we observed a rapid and progressive spreading of RFP^{+} cells from the meninges on the surface of the brain (8 hours after electroporation), alongside the projections of the meninges within the brain and via the choroid plexus (16-18 hours) to the lateral ventricles (24-48 hours) and thereafter into the cerebral cortex (Fig. 6B-G). RFP^{+} cells in the wall of the lateral ventricle appeared to form a stream of cells that was connected to and wrapped around the choroid plexus (Fig. 6G), suggesting that the choroid plexus served as a route via which meningeal cells migrated into the brain cortex. Interestingly, choroid plexi have been shown to orchestrate trafficking of other cell types (*i.e.,* leucocytes) into the brain [3], suggesting a broader role for the choroid

plexus as a gateway for different types of non-parenchymal cells to migrate inside the brain parenchyma.

Since RFP plasmid electroporation does not permanently label the transfected cells, we studied the long-term fate of the migrating meningeal cells by electroporating a Cre-expressing plasmid in the meninges of neonatal Rosa26-lox-stop-lox-YFP (Rosa26-YFP) mice [4]. Cre expression by transfected meningeal cells results in constitutive YFP expression, allowing long-term labeling and fate mapping of meningeal cells. At 7 and 30 days after Cre electroporation, YFP^+ cells were detected in the upper cerebral cortical layers I-IV and exhibited primarily a neuronal morphology (not shown). We quantified the fate of the YFP^+ meningeal-derived cells at postnatal day 30 when neuronal pruning had already occurred [5] (Table 1). Up to 77.3% of the parenchymal YFP^+ cells in the cortex showed a neuronal morphology and expressed the pan-neuronal marker NeuN, while 12.1% of YFP^+ cells expressed the astrocyte marker GFAP (not shown). YFP^+ cells did not express the oligodendrocyte precursor marker NG2 or the microglia marker Iba1 (not shown). Of the $NeuN^+$ cells, 71.9% expressed Satb2, a marker of excitatory neurons that establish callosal projections [6] (not shown), while 13.2% expressed the interneuron marker GAD65/67 (not shown). Thus, meningeal cells migrated into the brain parenchyma and generated primarily cortical neurons.

Radial glia cells are a well-established source of precursors for cerebral cortical neurons in the developing brain [7,8]. These cells, which can be labeled with the radial glia marker GLAST, surround the lateral ventricles (ventricular zone) in the developing brain [9]. An earlier study reported that a small population of cells expressing GLAST was detected in the meninges [10], though it is unknown whether these cells have similar neurogenic potential as radial glia. To examine whether the radially oriented RFP^+ cells in the cortex at 24 hours after electroporation were radial glia, we transfected the RFP reporter plasmid in meningeal cells via electroporation, and stained brain sections for the radial glia markers Blbp and GLAST. This analysis revealed that RFP^+ cells in the brain parenchyma did not express radial glia markers (Fig. 1H-J), except in rare cases (see next paragraph for possible explanation). To more convincingly assess whether the migrating meningeal cells were distinct from $GLAST^+$ radial glia cells and their progeny, we deployed radial glia cell-specific fate mapping. We therefore intercrossed the GLAST-Cre^{ERT2} mice (expressing the tamoxifen inducible Cre in radial glia cells) [11] with the Rosa26-lox-stop-lox-YFP reporter line [4] (yielding GLAST-YFP mice), resulting in permanent labeling of radial glia cells and their descendants upon tamoxifen injection [11]. To label radial glia cells and their progeny, we injected tamoxifen in P0 GLAST-YFP pups, while meningeal cells in the same pups were labeled via RFP electroporation. After 1 week, we detected YFP^+ cells in the ventricular and subventricular zone, and throughout the cortex. Consistent with the above mentioned report of a minor population of $GLAST^+$ cells in the meninges [10], we also observed a small population of YFP^+ cells in the meninges (7.9 ± 0.9% of all meningeal cells; n = 3). Since radial glia give rise to cortical neurons predominantly before birth and to glial cells after birth, almost none of the cortical YFP^+ cells expressed the pan-neuronal marker NeuN (not shown), suggesting that they were glial cells [11]. Notably, 92.2 ± 1.9% of the RFP^+ cells in the cortex were YFP^-, indicating that both cell populations were mostly non-overlapping and had a separate distinct origin (Fig. 6K; n = 3). We observed only some rare double RFP^+/YFP^+ cells in the cortex (not shown), which were possibly derived from the few YFP^+ meningeal cells upon electroporation of the RFP plasmid. Thus, in the cortex after birth, radial glia give rise mostly to non-neuronal cells, while meningeal cells give rise to neurons, the vast majority of which was not labeled by radial glia-specific fate mapping. The population of meningeal cells that migrated via the choroid plexus into the cortex was thus distinct from the population of cells derived from radial glia cells.

Birthdating experiments have shown that only a minimal number of dividing cells contributes to cortical neurogenesis after birth [9]. We assessed whether the cells that migrate from the meninges to the cortex at P0 were proliferating at the time of electroporation, and therefore exposed newborn pups to EdU 3 hours before RFP plasmid electroporation in the meninges. Analysis 48 hours later revealed only very

rare EdU^{+}/RFP^{+} cells in the brain parenchyma (4.3 ± 0.5%; n = 3), while EdU is not diluted out in proliferating cells at this timepoint [12], indicating that most migrating meningeal cells were not proliferating at the time of electroporation (Fig. 6L).

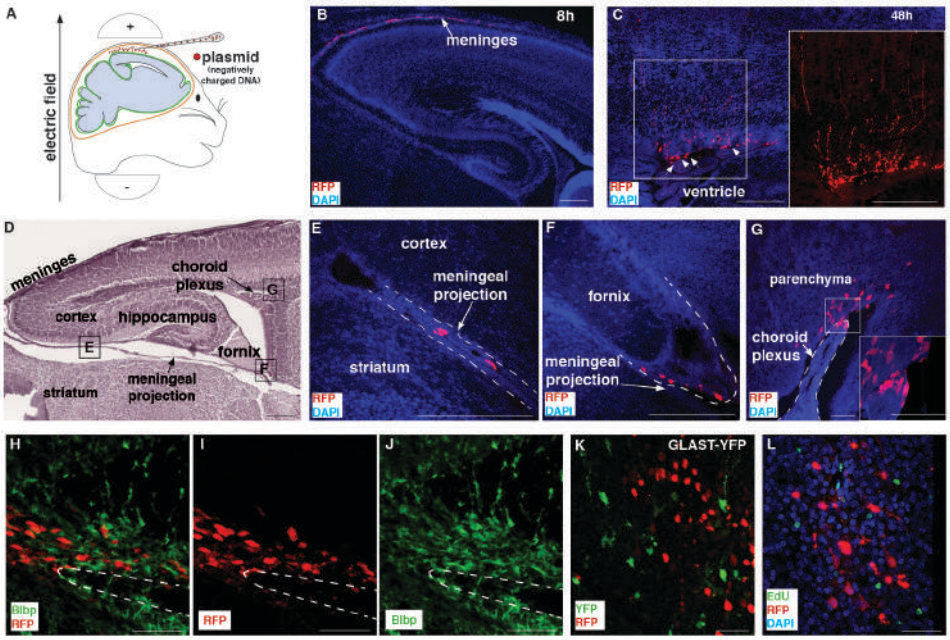

Figure 6: Meningeal cells migrate to the cortex and differentiate to neurons. A, Schematic representation of the electroporation of the RFP plasmid (denoted by red dots) in brain meninges after pressure-injection of the DNA into the subarachnoidal space. B,C, Sagittal brain section of P0 C57/BL6 wild type mice after electroporation of the meninges with the RFP plasmid, showing RFP+ cells in the meninges (arrows) at 8 hrs after electroporation (B); these RFP+ cells migrated to the ventricular and subventricular zone by 48 hrs after electroporation (C). Arrows in C point to RFP+ cells lining the ventricle. The inset in C shows the red color channel image of a larger magnification of the boxed area. D, H&E staining of a sagittal section through a P0 C57/BL6 mouse brain; the boxed areas (with letters inside) represent the brain location of the RFP+ cells shown in panels E-G. E-G, Sagittal brain section of P0 C57/BL6 mice upon electroporation of the meninges with the RFP expression plasmid showing the path of migration of RFP+ cells through the meningeal projection entering the brain (E), around the fornix (F) and the choroid plexus (G), at 18 hours after electroporation. Inset in G represents a higher magnification of the boxed area, showing RFP+ cells wrapping the choroid plexus. The dashed white lines in E-G delineate the meningeal projection (E,F), and choroid plexus (G). H-J, Brain section of a C57/BL6 P2 mouse electroporated with RFP plasmid at P0 and stained for the radial glia marker Blbp (green), showing that RFP+ cells do not co-express Blbp. Panel H shows the merged image; panel I and J show the single color channel images. The dashed white line delineates the ventricle. Single plane confocal images are shown. K, Staining of a brain section of a P2 GLAST-CreERT2 mouse crossed with the Rosa26-lox-stop-lox-YFP reporter line, 48 hours after tamoxifen injection (to induce radial glial cell specific YFP expression; GLAST-YFP) and RFP electroporation in the meninges, showing that YFP+ radial glia cells and RFP+ meningeal cells in the cortex each represent a separate non-overlapping population. L, Staining for EdU of a brain section of a C57/BL6 P2 mouse, 48 hours after RFP electroporation of the meninges and EdU administration, showing that RFP+ meningeal cells that migrated into the cortex were EdU-negative (non-proliferative). Panels C,E-G and K,L are maximum Z-projection images of confocal images, panels H-J show single plane confocal images, panel B is an epifluorescence microscope image. Scale bars: 200 μm (B-F), 50 μm (G-L).

To confirm whether the migration of neurogenic meningeal cells, observed in the electroporation experiments, also occurred physiologically in unperturbed conditions (*i.e.*, in a model in which meningeal cells were not transfected via electroporation), we employed a gene fate mapping strategy, taking profit from a Wnt1-Cre driver strategy for the following reasons. Since forebrain meningeal pericytes and stromal cells are derived from neural crest cells and express Wnt1 from early embryonic development onwards [13-15], we intercrossed a Wnt1-Cre driver line [16] with a Rosa26-lox-stop-lox-YFP reporter line [4] (yielding Wnt1-YFP mice), resulting in permanent labeling of Wnt1-expressing cells and its descendants. In agreement with previous observations [13], we detected YFP expression in E16 embryos and P0 pups in the diencephalon, hippocampus, forebrain meninges, meningeal brain

projections as well as in brain pericytes (Fig. 7A-E). Wnt1-YFP$^+$ cells were found to be wrapping and lining the choroid plexus. Notably, we also observed Wnt1-YFP$^+$ cells, arranged in columns of radially oriented cells in the cerebral cortex, spanning from the ventricle to the upper cortical layers (Fig. 7B). These cells in the brain of P0 pups expressed markers of neuronal precursors, i.e. HuC/D and doublecortin (not shown). In P15 and adult Wnt1-YFP mice, we observed a similar distribution of Wnt1-YFP$^+$ cells, however the columns of Wnt1-YFP$^+$ cells in the cortex were no longer detectable in the ventricular and subventricular zone, but became restricted to the upper cortical layers I to IV (not shown). Up to 82.7% of the cortical Wnt1-YFP$^+$ cells in adult mice showed a typical neuronal morphology and expressed the pan-neuronal marker NeuN (Fig. 7F-H; Table1). Another 5.2% of the Wnt1-YFP$^+$ cells were GFAP$^+$ astrocytes and 5.7% were NG2$^+$ oligodendrocyte precursors or pericytes (Table 1). No Iba1$^+$ cells were observed amongst the Wnt1-YFP$^+$ cells (Table 1). Of the NeuN$^+$ cells, 60.8% expressed Satb2 (Fig. 7F-H), while 12.1% expressed GAD65/67 (Table 1). The results obtained using the unperturbed Wnt1-YFP mouse model showed that a fraction of the Wnt1-YFP$^+$ cells generated cortical neurons. Moreover, the distribution of Wnt1-YFP$^+$ cells in the meninges, meningeal projections of the brain and choroid plexi very closely resembled the pattern of labeled cells observed in the RFP electroporation experiments (Fig. 6B-G; Fig. 7A,B), and therefore suggested a possible meningeal origin of the Wnt1-YFP$^+$ cortical neurons. However, since other cell types in the brain also expressed Wnt1, this experiment did not exclude the possibility that Wnt1-YFP$^+$ cortical neurons originated from other Wnt1-YFP$^+$ cells in non-meningeal brain regions.

Table1

Mouse line	Gene transfer	Vector	Tamox	Cre$^+$ cells	NeuN$^+$ cells	GFAP$^+$ cells	NG2$^+$ cells	Iba1$^+$ cells	NeuN$^+$ cells expressing neuronal markers	
									Satb2$^+$	GAD65/67$^+$
Rosa26-YFP	EP	Cre	n.a.	n.a.	77.3 ± 3.4 (n=4)	12.1 ± 2.9 (n=4)	0 ± 0 (n=3)	0 ± 0 (n=3)	55.6 ± 2.2 (n=3) 71.9± 2.2*	10.2 ± 0.5 (n=3) 13.2± 0.5*
Wnt1-YFP	n.a.	n.a.	n.a.	n.a.	82.7± 1.1 (n=4)	5.2± 0.3 (n=4)	5.7± 1.4 (n=4)	0 ± 0 (n=4)	50.3± 4.6 (n=4) 60.8± 4.6*	10.0± 1.7 (n=6) 12.1± 1.7*
WT	LV	Brainbow 1.0(L)	n.a.	19.6 ± 2.4 (n=5)	n.a.	n.a.	n.a.	n.a.	n.a.	n.a.
Wnt1-Cre	LV	Brainbow 1.0(L)	n.a.	70.2 ± 2.9 (n=6)	72.7± 1.2 (n=6)	13.9 ± 1.7 (n=4)	0.5 ± 0.5 (n=5)	0 ± 0 (n=4)	48.0± 3.9 (n=4) 66.0± 3.9*	4.9 ± 1.2 (n=4) 6.7± 1.2*
SOX10-Cre^{ERT2}	LV	Brainbow 1.0(L)	P0	67.6 ± 7.9 (n=4)	72.8 ± 5.4 (n=4)	9.8 ± 2.9 (n=4)	0.5 ± 0.5 (n=4)	0 ± 0 (n=4)	46.1 ± 3.6 (n=4) 63.3 ± 3.6*	14.0 ± 0.4 (n=4) 19.2 ± 0.4*
PDGFRβ−Cre	LV	Brainbow 1.0(L)	n.a.	76.7 ± 1.6 (n=5)	82.2 ± 1.1 (n=4)	10.4 ± 3.8 (n=4)	1.0 ± 1.0 (n=4)	0 ± 0 (n=4)	70.7 ± 5.3 (n=5) 86.0 ± 5.3*	11.0 ± 1.1 (n=5) 13.4 ± 1.1*
VE-cadherin (PAC)-Cre^{ERT2}	LV	Brainbow 1.0(L)	P0	18.8 ± 2.7 (n=3) #	n.a.	n.a.	n.a.	n.a.	n.a.	n.a.

TABLE 1: Quantitative analysis of the meningeal-derived cells in the cortex of p30 mice. Numbers are expressed as percentage of the total number of cells counted (for Wnt1Cre-YFP and Rosa26-YFP mouse lines: YFP+ cells; for all other mouse lines: CFP+, YFP+ and dtT+ cells), or when indicated by an asterisk (*) as a percentage of the NeuN+YFP+ cells (for Wnt1Cre-YFP and Rosa26-YFP mouse lines) or of the NeuN+YFP+ and NeuN+CFP+ cells (recombined Brainbow 1.0(L) cells for the other mouse lines). For unknown reasons the Brainbow reporter 1.0(L) showed spontaneous excision of tdTomato and induction of CFP and YFP even without the presence of Cre (this was observed also following cell transduction in vitro), as was the case in the meninges of Cre-negative mice (WT) or of mice, in which no contribution of meningeal cells to cortical cells was visualized (endothelial cell specific VE-cadherin(PAC)-CreERT2 mice). This background activation of the Brainbow 1.0(L) reporter, assessed by counting the fraction of YFP+ plus CFP+ cells (% of YFP+, CFP+ and tdTomato+ cells) was ca 19%, thus much lower than the >70% values that we obtained in the mouse strains expressing active Cre. Data are expressed as mean ± SEM. n.a.: not applicable; Tamox: tamoxifen (the day of administration is indicated); GFAP: astrocyte marker glial fibrillary acidic protein; NG2: oligodendrocyte progenitor and pericyte marker neural/glial antigen 2; Iba1: microglia marker ionized calcium-binding adapter molecule 1; Satb2: excitatory neuron marker special AT-rich sequence-binding protein 2; GAD65/67: GABA-ergic interneuron marker glutamic acid decarboxylase 65/67; EP: electroporation; LV: lentiviral transduction.

#: P=NS vs WT and P<0.005 vs all other lines. Cre+ cells: cells in which the Brainbow 1.0(L) reporter was recombined and yielded YFP+ plus CFP+ cells.

To explore whether Wnt1-YFP$^+$ cortical neurons originated from neural crest-derived meningeal cells, we devised a technique to selectively label only the Wnt1-expressing cells in the meninges. We therefore injected a lentiviral vector expressing the Brainbow reporter 1.0(L) in the meninges of P0 Wnt1-Cre mice. This Brainbow 1.0(L) reporter is engineered such that it expresses tdTomato before, and CFP or YFP after Cre-mediated excision of the floxed stop cassette [17] (Fig. 7I). To reliably obtain sensitive detection of the FPs, we amplified the weak FP signal by immunostaining using an antibody recognizing tdTomato (yielding red color) and another one crossreacting with CFP and YFP (yielding green colour). Once switched on, the persistent expression of the CFP and YFP allows fate mapping of the Wnt1-expressing meningeal cells and their progeny. Since tdTomato-labeled cells represent cells in which Cre was not active, we focused on the cells expressing CFP and YFP. For unknown reasons, we observed background recombination, leading to the formation of 19.6% CFP$^+$ and YFP$^+$ cortical cells in wild type (WT) mice, not expressing Cre (Table 1). A similar background activation of the Brainbow 1.0(L) was observed when transducing this reporter in cultured cells (not shown). Similar to what we observed in Rosa26-YFP mice electroporated with the Cre plasmid, analysis of Wnt1-Cre mice, 1 month after lentiviral transduction with the Brainbow 1.0(L) reporter in the meninges, revealed the presence of substantial numbers of CFP$^+$ and YFP$^+$ cortical cells (70.2 % of all labeled cells) in the upper cortical layers I to IV (Fig. 7J; Table 1). Of those, 72.7% showed a typical neuronal morphology and expressed NeuN (Fig. 7K-M). Another fraction of the CFP$^+$ and YFP$^+$ cortical cells (13.9%) had a non-neuronal morphology and expressed GFAP (Table 1). NG2$^+$ and Iba1$^+$ cells were respectively, minimally or not detected amongst the CFP$^+$ and YFP$^+$ cortical cells (Table 1). Of the CFP$^+$ and YFP$^+$ neurons (NeuN$^+$), up to 66.0% expressed Satb2, while 6.7% expressed GAD65/67 (Table 1). Overall, Wnt1-expressing meningeal cells generated cortical neurons in the adult brain. To further confirm the neural crest origin of the neurogenic meningeal cells and to conditionally induce genetic labeling of the neural crest cells of the meninges, we employed the Sox10-Cre^{ERT2} mouse line [18], since Sox10 marks these neural crest cells [19]. We injected tamoxifen in P0 Sox10-Cre^{ERT2} mice followed by transduction of the meninges with the lentiviral vector expressing Brainbow 1.0(L). Consistent with our other results, we observed substantial numbers of CFP$^+$ and YFP$^+$ cells in the cerebral cortex (67.6% of labeled cells) (Table 1), of which 72.8% expressed NeuN (Table1). As shown in Table 1, 9.8% of the CFP$^+$ and YFP$^+$ cortical cells expressed GFAP, while NG2$^+$ and Iba1$^+$ cells were respectively, minimally or not detected amongst the CFP$^+$ and YFP$^+$ cortical cells (Table 1). Up to 63.3% of the CFP$^+$ and YFP$^+$ neurons expressed Satb2, while 19.2% expressed GAD65/67 (Fig. 7N-P; Table 1). Hence, neural crest-derived cells of the meninges generated cortical neurons.

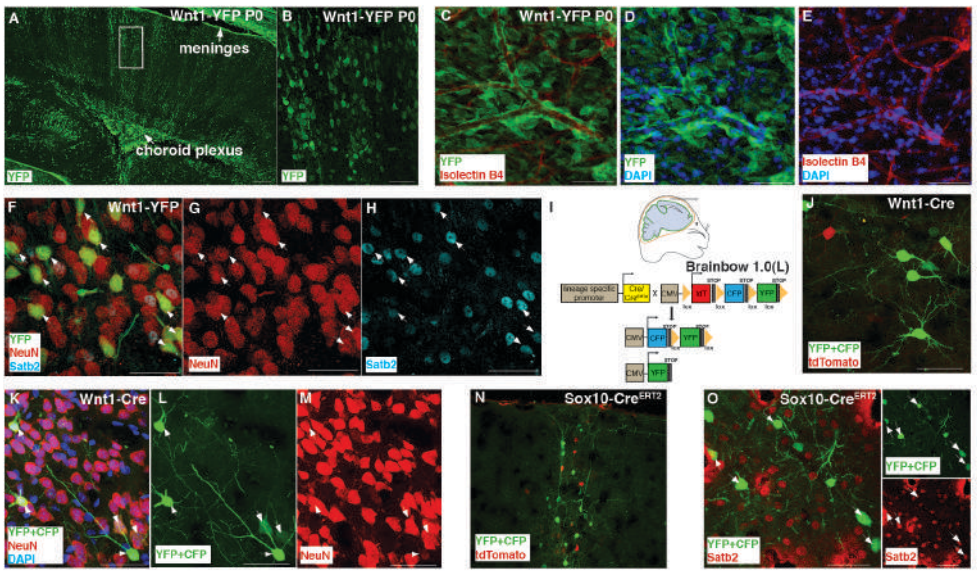

Figure 7: Neural crest origin of neurogenic meningeal cells. A,B, Staining of a 30 µm-thick brain section of a P0 pup from an intercross of Wnt1-Cre mice with Rosa26-lox-stop-lox-YFP mice (Wnt1-YFP), showing the distribution of YFP+ cells in columns in the dorsal cortex, meninges and choroid plexi (arrows). Panel B represents a higher magnification of the boxed area in A showing the presence of YFP+ cells in cortical columns. C-E, Whole mount staining of brain meninges of a Wnt1-YFP P0 pup for YFP and isolectin B4 (endothelial cell marker), showing that at least a fraction of the YFP+ cells is in close contact with the blood vessels (arrowheads; top view). Panels C-E show the merged images for the indicated different color combinations. F-H, Triple staining of a cerebral cortex section of a P30 Wnt1-YFP mouse for the pan-neuronal marker NeuN, the excitatory neuron marker Satb2 and YFP, showing YFP+ excitatory neurons co-expressing Satb2 and NeuN (arrows in F-H). Merged image is shown in F; single color channel images in G,H. I, Schematic representation of the Cre induced recombination of the Brainbow 1.0(L) reporter expressed by a lentiviral vector injected in the meninges of lineage-specific Cre(ERT2) expressing mice. The red/brown and green line in the brain scheme denotes the outer layer and inner layer (pia mater) of the meninges, respectively. The different colors after Cre-recombination are shown. CFP, cerulean fluorescent protein; tdT, tdTomato fluorescent protein; YFP, yellow fluorescent protein; CMV, cytomegalovirus promoter. J, Brain cortex of a P30 Wnt1-Cre mouse, injected in the meninges with a lentiviral vector expressing the Brainbow1.0(L) reporter at P0, and stained for YFP/CFP and tdTomato, showing that the meningeal derived-cells that have migrated into cortical layer I-IV are mostly Wnt1_Cre derived YFP+/CFP+ (green; Cre active) cells. K-M, Brain section of a P30 Wnt1-Cre mouse, in which a lentiviral vector expressing the Brainbow 1.0(L) reporter was injected in the meninges at P0, stained for the pan-neuronal marker NeuN and YFP/CFP (arrows in K-M), showing the presence of YFP+/CFP+ cells (green; Cre active) in the cortex; these cells exhibited a typical neuronal morphology and expressed NeuN (arrows). Panel K shows merged image; panels L,M show the respective single color channel images. N-P, Brain section of a P30 Sox10-CreERT2 mouse, in which a lentiviral vector expressing the Brainbow 1.0(L) reporter was injected in the meninges at P0, stained for Satb2 and YFP/CFP, showing that YFP+/CFP+ cells (green) in the cortex were mostly Satb2+ excitatory neurons (arrows). The left micrograph shows merged image; the right microgrpahs show the respective single color channel images. Cell nuclei are visualized by DAPI staining. All micrographs are maximum Z-projections of confocal images. Scale bars: 200 μm (A), 50 μm (B-P

Wnt1-YFP$^+$ meningeal cells showed a perivascular distribution (Fig. 7C-E). Meninges are a highly vascularized tissue, containing blood vessels that are in close contact with perivascular cells expressing PDGFRß [20]. In fact, 24.2 ± 2.0% of the meningeal cells expressed this marker (Fig. 8A-C; n = 3). We therefore explored whether the neurogenic cells in the meninges were PDGFRß$^+$ perivascular cells. We set out to map the genetic fate of these cells by injecting the Brainbow 1.0(L) vector in the meninges of newborn PDGFRß-Cre mice [21] (see scheme in Fig. 7I). Fate analysis at 1 month after Brainbow 1.0(L) lentiviral transduction showed CFP$^+$ and YFP$^+$ cells in the upper cortical layers I to IV (76.7% of all labeled cells) (Fig. 8D), of which 82.2% expressed NeuN (Fig. 8E,F; Table 1). As shown in Table 1, 10.4% of the CFP$^+$ and YFP$^+$ cells in the cortex expressed GFAP (Table 1). NG2$^+$ and Iba1$^+$ cells were respectively, minimally or not detected amongst the CFP$^+$ and YFP$^+$ cortical cells (Table 1). As shown in Table 1, most of the CFP$^+$ and YFP$^+$ neurons were excitatory in nature and expressed Satb2 (86.0%) (Fig. 8E-G), while a small proportion were GAD65/67$^+$ interneurons (13.4%). Taken together, perivascular PDGFRß$^+$ cells can migrate from their meningeal location into the brain parenchyma and differentiate primarily to excitatory neurons in the upper layer I-IV of the cortex.

In the Wnt1-Cre, Sox10-Cre^{ERT2} and PDGFRß-Cre lines transduced with Brainbow 1.0(L), ~ 25-30% of the labeled cortical cells were tdTomato$^+$, indicating that Cre was not active in these cells at the time of the transduction. This may suggest that even though all labeled meningeal cells were neurogenic, they did not uniformly express – at least at the time of transduction – Wnt1, Sox10 or PDGFRß.

Our results show that PDGFRß$^+$ perivascular meningeal cells can give rise to cortical neurons in the postnatal mouse brain. These meningeal neurogenic cells are distinct from the well-characterized neurogenic parenchymal radial glia and, given their Wnt1/Sox10 expression, likely are of neural crest origin (Fig. 8H). It was already known that cephalic neural crest-derived cells can enter the forebrain early in development to differentiate mostly to PDGFRß$^+$ pericytes [14]. Here we show that meningeal PDGFRß$^+$ perivascular cells can also migrate to the cortex to differentiate to neurons postnatally. These findings are relevant for multiple reasons: *i*) they expand the notion that postnatal brain neurogenesis is restricted to rare germinative remnants of the neuroepithelium; *ii*) they broaden the concept of brain plasticity; and *iii*) they challenge the dogma that only parenchymal cells can contribute to neurogenesis, highlighting the importance of vascular cells as a reservoir of neurogenic cells.

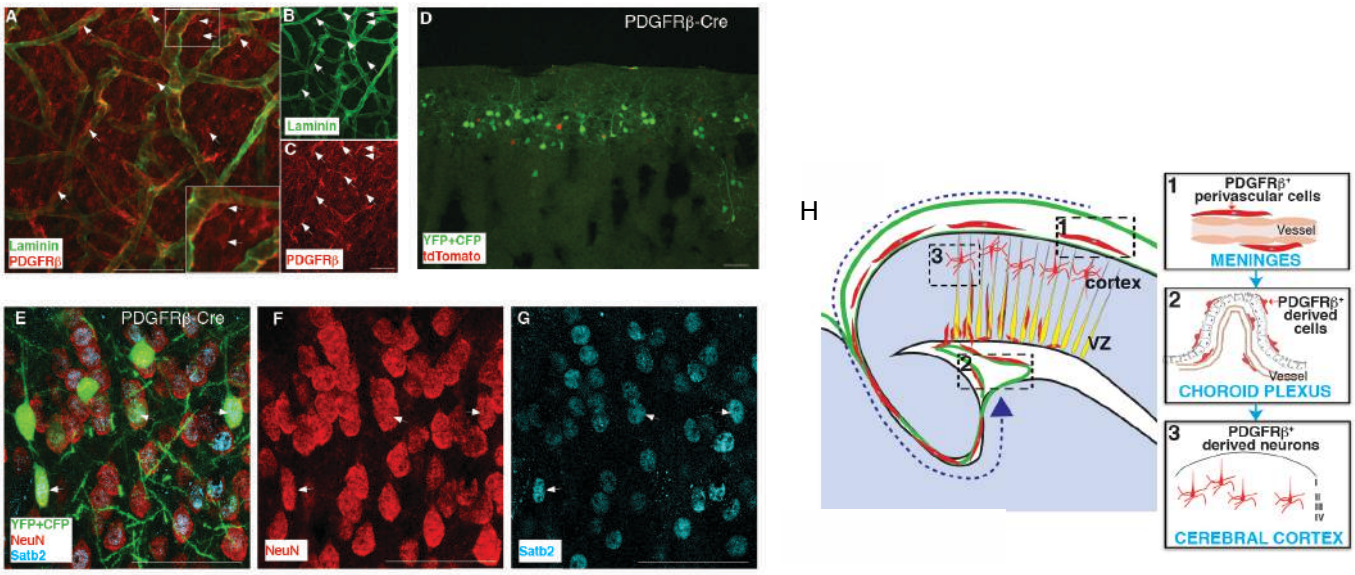

Figure 8: Pdgfrß+ perivascular meningeal cells generate cortical neurons A-C, Whole mount staining for laminin (to visualize blood vessels) and PDGFRß (to visualize perivascular cells) of the brain meninges of a P0 C57/BL6 pup (top view), showing the presence of numerous PDGFRß+ cells in close contact with the vessels of the brain meninges (arrows in A,C denote PDGFRß+ cells and in B refer to their localization on laminin). Inset in A is a higher magnification of the boxed area. Panel A shows merged image; panels B,C show the respective single color channel images D, Brain cortex of a P30 PDGFRß-Cre mouse, injected at P0 with a lentiviral vector expressing the Brainbow 1.0(L) reporter in the meninges (see scheme in Fig. 2I), stained for YFP/CFP and tdTomato, showing that the meningeal cells that migrated into the cortical layer I-IV were mostly PDGFRß_Cre derived YFP+/CFP+ (green) cells. E-G, Brain cortex of a P30 PDGFRß-Cre mouse, injected at P0 with the lentiviral vector expressing Brainbow 1.0(L) reporter in the meninges, stained for YFP/CFP (E), Satb2 (E,G), and NeuN (E,F), showing that most meningeal cells that migrated into the cortical layers I-IV were Satb2+ excitatory neurons (arrows in E-G). Panel E shows merged image; panels F,G show the single red or blue color channel images. H, Scheme of the proposed model for meningeal perivascular cell migration and differentiation: meningeal PDGFRß+ cells (red) (box 1) migrate to the cortex via the choroid plexus (box 2) and differentiate to neurons (box 3). These PDGFRß+ meningeal neurogenic cells are distinct from the neurogenic radial glia (yellow). The large dashed blue arrow in H indicates the path of migration of meningeal neurogenic cells to the cortex. The green line denotes meninges and their brain projections. VZ: ventricular zone. All micrographs are maximum Z-projections of confocal images. Scale bars: 50 μm

REFERENCES

1 Zhang, J. *et al.* UCP2 regulates energy metabolism and differentiation potential of human pluripotent stem cells. *The EMBO journal* **30**, 4860-4873, doi:10.1038/emboj.2011.401 (2011).

2 De Bock, K. *et al.* Role of PFKFB3-driven glycolysis in vessel sprouting. *Cell* **154**, 651-663, doi:10.1016/j.cell.2013.06.037 (2013).

3 Shechter, R. *et al.* Recruitment of beneficial M2 macrophages to injured spinal cord is orchestrated by remote brain choroid plexus. *Immunity* **38**, 555-569, doi:10.1016/j.immuni.2013.02.012 (2013).

4 Srinivas, S. *et al.* Cre reporter strains produced by targeted insertion of EYFP and ECFP into the ROSA26 locus. *BMC developmental biology* **1**, 4 (2001).

5 Bandeira, F., Lent, R. & Herculano-Houzel, S. Changing numbers of neuronal and non-neuronal cells underlie postnatal brain growth in the rat. *Proceedings of the National Academy of Sciences of the United States of America* **106**, 14108-14113, doi:10.1073/pnas.0804650106 (2009).

6 Alcamo, E. A. *et al.* Satb2 regulates callosal projection neuron identity in the developing cerebral cortex. *Neuron* **57**, 364-377, doi:10.1016/j.neuron.2007.12.012 (2008).

7 Doetsch, F., Caille, I., Lim, D. A., Garcia-Verdugo, J. M. & Alvarez-Buylla, A. Subventricular zone astrocytes are neural stem cells in the adult mammalian brain. *Cell* **97**, 703-716 (1999).

8 Kriegstein, A. & Alvarez-Buylla, A. The glial nature of embryonic and adult neural stem cells. *Annual review of neuroscience* **32**, 149-184, doi:10.1146/annurev.neuro.051508.135600 (2009).
9 Gage, F. H. & Temple, S. Neural stem cells: generating and regenerating the brain. *Neuron* **80**, 588-601, doi:10.1016/j.neuron.2013.10.037 (2013).
10 Berger, U. V. & Hediger, M. A. Distribution of the glutamate transporters GLAST and GLT-1 in rat circumventricular organs, meninges, and dorsal root ganglia. *The Journal of comparative neurology* **421**, 385-399 (2000).
11 Mori, T. *et al.* Inducible gene deletion in astroglia and radial glia--a valuable tool for functional and lineage analysis. *Glia* **54**, 21-34, doi:10.1002/glia.20350 (2006).
12 Fei, J. F. & Huttner, W. B. Nonselective sister chromatid segregation in mouse embryonic neocortical precursor cells. *Cerebral cortex* **19 Suppl 1**, i49-54, doi:10.1093/cercor/bhp043 (2009).
13 Jiang, X., Iseki, S., Maxson, R. E., Sucov, H. M. & Morriss-Kay, G. M. Tissue origins and interactions in the mammalian skull vault. *Developmental biology* **241**, 106-116, doi:10.1006/dbio.2001.0487 (2002).
14 Yamanishi, E., Takahashi, M., Saga, Y. & Osumi, N. Penetration and differentiation of cephalic neural crest-derived cells in the developing mouse telencephalon. *Development, growth & differentiation* **54**, 785-800, doi:10.1111/dgd.12007 (2012).
15 Sauka-Spengler, T. & Bronner-Fraser, M. Evolution of the neural crest viewed from a gene regulatory perspective. *Genesis* **46**, 673-682, doi:10.1002/dvg.20436 (2008).
16 Chai, Y. *et al.* Fate of the mammalian cranial neural crest during tooth and mandibular morphogenesis. *Development* **127**, 1671-1679 (2000).
17 Livet, J. *et al.* Transgenic strategies for combinatorial expression of fluorescent proteins in the nervous system. *Nature* **450**, 56-62, doi:10.1038/nature06293 (2007).
18 Simon, C., Lickert, H., Gotz, M. & Dimou, L. Sox10-iCreERT2 : a mouse line to inducibly trace the neural crest and oligodendrocyte lineage. *Genesis* **50**, 506-515, doi:10.1002/dvg.22003 (2012).
19 Website. Allen Developing Mouse Brain Atlas [Internet]. (2013).
20 Lindahl, P., Johansson, B. R., Leveen, P. & Betsholtz, C. Pericyte loss and microaneurysm formation in PDGF-B-deficient mice. *Science* **277**, 242-245 (1997).
21 Foo, S. S. *et al.* Ephrin-B2 controls cell motility and adhesion during blood-vessel-wall assembly. *Cell* **124**, 161-173, doi:Doi 10.1016/J.Cell.2005.10.034 (2006).

SUMMARY PROGRESS OF THE RESEARCHER TRAINING/TRANSFER OF KNOWLEDGE ACTIVITIES

The research proposal is focused on the characterization and modulation of the meningeal stem perivascular cell (MeSP) activation and differentiation. The research training primarily concentrates on: *(i)* acquiring knowledge and expertise in the generation and manipulation of transgenic animals; and *(ii)* acquiring advanced knowledge on the metabolic analysis using radioisotopes.

(i) Acquiring knowledge and expertise in animal transgenesis

The researcher has been able to generate and maintain Wnt1-Cre:YFP; PDGFRß-Cre:YFP; PDGFrßCRE x PFKFB3lox/lox; NG2CRE ERT2 PFKFB3lox/lox those lines were mentioned in the results report. Moreover the researcher generated, maintained and screened meningeal recombination also in the following lines NestinCRE-ERT2:YFP, GLASTCRE-ERT2:YFP PDGFralphaCRE-ERT2:YFP, SOXCRE-ERT2:YFP

(ii) Acquiring advanced knowledge in metabolic analysis

The researcher has spent a great deal of time learning and mastering techniques for metabolic flux analysis using either radioisotope-labeled metabolites and analysis by scintillation counter or stable isotope-labeled metabolites in conjunction with analysis by Gas Chromatography Mass Spectrometry (GC-MS).

Further training of the researcher has also included acquiring skills such as *(i)* coordination and management of resources, people and collaborators; *(ii)* awareness of ethical issues in animal-based studies; and *(iii)* writing grant applications and scientific publications, as well as presenting of the results at meetings and conferences. The researcher has been actively involved in training activities that will

be very important for her future career as a young group leader. She has participated in the writing and revision of grants and papers for the host laboratory. She is also collaborating with other research projects of the host laboratory, integrating her knowledge and expertise with them. Moreover, the researcher is supervising one PhD student.

SIGNIFICANT RESULTS

Manuscript submitted

Ilaria Decimo*, Francesco Bifari*, Annachiara Pino, Christian Lange, Stefan Vinckier, Sabine Wyns, Leda Dimou, Mieke Dewerchin & Peter Carmeliet. Perivascular meningeal cells contribute to cortical neurogenesis in the mammalian brain. *Science under revision*

Annelies Quaegebeur, **Ilaria Decimo**, Sandra Schoors, Bart Ghesquière, Francesco Bifari, Sudha Rani Janaki Raman, Gitte Borgers, Bert Cruys, Carla De Legher, Ann Bouché, Luc Schoonjans, Matt S. Ramer, Gene Hung, Don W.Cleveland, Robin Lemmens, Wim Robberecht, C. Frank Bennett, Katrien DeBock, Sarah-Maria Fendt,, Mieke Dewerchin & Peter Carmeliet, Deletion or inhibition of the oxygen sensor phd1 protects against ischemic stroke via reprogramming of neuronal metabolism. *Cell Metabolism under revision*

Christian Lange, Miguel Turrero Garcia, **Ilaria Decimo**, Francesco Bifari, Guy Eelen, Annelies Quaegebeur, Ruben Boon, Hui Zhao, Bram Boeckx, Junlei Chang, Christine Wu, Ferdinand Le Noble, Diether Lambrechts, Mieke Dewerchin,Calvin J. Kuo, Wieland B. Huttner & Peter Carmeliet. Relief of physiological hypoxia by formation of niche blood vessels promotes neural stem cell differentiation during cerebral cortex development. *Developmental Cell submitted*

Manuscript in preparation

Anna Rita Cantelmo, Aleksandra Brajic, Joanna Kalucka, Jermaine Goveia, Ann Bouché, Ivo Cornelissen, Stefan Vinckier, Sandra Schoors, Koen Veys, Kim Kampen4, Katrien De Bock3, Francesco Bifari, Peter Stapor, **Ilaria Decimo,** Mieke Dewerchin & Peter Carmeliet. Partial reduction of glycolysis by pfkfb3-blockade induces tumor vessel normalization and impairs metastasis. *Cancer Cell in preparation.*

Published article

Schoors S*, Cantelmo AR*, Georgiadou M*, Stapor P, Wang X, Wong BW, Bifari F, Quaegebeur A, **Decimo I,** Schoonjans L, De Bock K, Dewerchin M, Carmeliet P. Incomplete and transitory decrease of glycolysis: A new paradigm for anti-angiogenic therapy? *Cell Cycle*. 2013 Dec 13;13(1). [Impact factor – 5.243]

De Bock K*, Georgiadou M*, Schoors S, Kuchnio A, Wong BW, Cantelmo AR, Quaegebeur A, Ghesquière B, Cauwenberghs S, Eelen G, Phng LK, Betz I, Tembuyser B, Brepoels K, Welti J, Geudens I, Segura I, Cruys B, Bifari F, **Decimo I**, Blanco R, Wyns S, Vangindertael J, Rocha S, Collins RT, Munck S, Daelemans D, Imamura H, Devlieger R, Rider M, Van Veldhoven PP, Schuit F, Bartrons R, Hofkens J, Fraisl P, Telang S, Deberardinis RJ, Schoonjans L, Vinckier S, Chesney J, Gerhardt H, Dewerchin M, Carmeliet P. Role of PFKFB3-driven glycolysis in vessel sprouting. *Cell*. 2013; 154: 651-663. [Impact factor – 31.957]

Abstract presented:

Ilaria Decimo*, Francesco Bifari*, Annachiara Pino, Christian Lange, Stefan Vinckier, Sabine Wyns, Leda Dimou, Mieke Dewerchin & Peter Carmeliet. Perivascular meningeal cells contribute to cortical

neurogenesis in the mammalian brain. IAP « WIBRAIN » Spring meeting, April 23rd 2015, Brussel Belgium (Oral presentation)